

Multimodal Characterization of the Late Effects of Traumatic Brain Injury: A Methodological Overview of the Late Effects of Traumatic Brain Injury Project

Brian L. Edlow,^{1,2} C. Dirk Keene,³ Daniel P. Perl,^{4,5} Diego Iacono,^{4–7} Rebecca D. Folkerth,^{8,9} William Stewart,¹⁰ Christine L. Mac Donald,¹¹ Jean Augustinack,² Ramon Diaz-Arrastia,¹² Camilo Estrada,¹³ Elissa Flannery,¹⁴ Wayne A. Gordon,¹⁴ Thomas J. Grabowski,^{15,16} Kelly Hansen,¹³ Jeanne Hoffman,¹⁷ Christopher Kroenke,¹⁸ Eric B. Larson,¹³ Patricia Lee,^{4,7} Azma Mareyam,² Jennifer A. McNab,¹⁹ Jeanne McPhee,¹⁴ Allison L. Moreau,² Anne Renz,¹³ Katie Rose Richmire,¹³ Allison Stevens,² Cheuk Y. Tang,²⁰ Lee S. Tirrell,² Emily H. Trittschuh,^{21,22} Andre van der Kouwe,² Ani Varjabedian,² Lawrence L. Wald,² Ona Wu,² Anastasia Yendiki,² Liza Young,¹⁶ Lilla Zöllei,² Bruce Fischl,² Paul K. Crane,²³ and Kristen Dams-O'Connor^{14,24}

Abstract

Epidemiological studies suggest that a single moderate-to-severe traumatic brain injury (TBI) is associated with an increased risk of neurodegenerative disease, including Alzheimer's disease (AD) and Parkinson's disease (PD). Histopathological studies describe complex neurodegenerative pathologies in individuals exposed to single moderate-to-severe TBI or repetitive mild TBI, including chronic traumatic encephalopathy (CTE). However, the clinicopathological links between TBI and post-traumatic neurodegenerative diseases such as AD, PD, and CTE remain poorly understood. Here, we describe the methodology of the Late Effects of TBI (LETBI) study, whose goals are to characterize chronic post-traumatic neuropathology and to identify *in vivo* biomarkers of post-traumatic neurodegeneration. LETBI participants undergo extensive clinical evaluation using National Institutes of Health TBI Common Data Elements, proteomic and genomic analysis, structural and functional magnetic resonance imaging (MRI), and prospective consent for brain donation. Selected brain specimens undergo ultra-high resolution *ex vivo* MRI and histopathological evaluation including whole-mount analysis. Co-registration of *ex vivo* and *in vivo* MRI data enables identification of *ex vivo* lesions that were present during life. *In vivo* signatures of postmortem pathology are then correlated with cognitive and behavioral data to characterize the clinical phenotype(s) associated with pathological brain lesions. We illustrate the study methods and demonstrate proof of concept for this approach by reporting results from the first LETBI participant, who despite the presence of multiple *in vivo* and *ex vivo* pathoanatomic lesions had normal cognition and was functionally independent until her mid-80s. The LETBI project

¹Department of Neurology, Massachusetts General Hospital and Harvard Medical School, Boston, Massachusetts.

²Athinoula A. Martinos Center for Biomedical Imaging, Department of Radiology, Massachusetts General Hospital and Harvard Medical School, Charlestown, Massachusetts.

³Department of Pathology, ¹¹Department of Neurological Surgery, ¹⁵Department of Neurology, ¹⁶Department of Radiology, ¹⁷Department of Rehabilitation Medicine, ²¹Department of Psychiatry and Behavioral Sciences, ²⁵Department of Medicine, University of Washington, Seattle, Washington.

⁴Brain Tissue Repository and Neuropathology Core, ⁵Department of Pathology, ⁶Department of Neurology, Uniformed Services University of the Health Sciences, Bethesda, Maryland.

⁷The Henry M. Jackson Foundation for the Advancement of Military Medicine, Bethesda, Maryland.

⁸Department of Pathology, Brigham and Women's Hospital, Harvard Medical School, Boston, Massachusetts.

⁹City of New York Office of the Chief Medical Examiner and New York University School of Medicine, New York, New York.

¹⁰Department of Neuropathology, Queen Elizabeth University Hospital and Institute of Neuroscience and Psychology, University of Glasgow, United Kingdom.

¹²Department of Neurology and Center for Brain Injury and Repair, Hospital of the University of Pennsylvania, Philadelphia.

¹³Kaiser Permanente Washington Health Research Institute, Seattle, Washington.

¹⁴Department of Rehabilitation Medicine, ²⁰Department of Radiology, ²⁴Department of Neurology, Icahn School of Medicine at Mount Sinai, New York, New York.

¹⁸Advanced Imaging Research Center, Oregon Health and Science University, Portland, Oregon.

¹⁹Department of Radiology, Stanford University, Stanford, California.

²²Geriatric Research Education and Clinical Center, VA Puget Sound Health Care System, Seattle, Washington.

represents a multidisciplinary effort to characterize post-traumatic neuropathology and identify *in vivo* signatures of postmortem pathology in a prospective study.

Keywords: dementia; MRI; neurodegeneration; neuropathology; traumatic brain injury

Introduction

TRAUMATIC BRAIN INJURY (TBI) may be associated with an increased risk of neurodegenerative disease, including Alzheimer's disease (AD), Parkinson's disease (PD), and chronic traumatic encephalopathy (CTE).¹⁻⁵ However, these outcomes affect only a portion of long-term TBI survivors, and the pathogenesis, clinical phenotypes, and neuropathological signatures of post-traumatic neurodegeneration are incompletely understood.⁶⁻⁸ Similarly, the mechanistic link between postmortem pathology and clinical symptoms is undefined. Limited knowledge of the neurodegenerative sequelae of TBI has precluded the identification of *in vivo* biomarkers of TBI-associated neurodegeneration, which impedes the development of targeted therapies.

Here, we describe the methods of a prospective, multi-institutional study, the Late Effects of TBI (LETBI) project, which aims to advance understanding of the behavioral characteristics, imaging biomarkers, pathophysiology, and neuropathological signatures associated with post-traumatic conditions that follow a single moderate or severe TBI or multiple mild TBI. The conceptual basis for the LETBI project is that prospective acquisition and multimodal integration of neurobehavioral, neuroimaging, and neuropathological data in large, well-characterized samples are essential for advancing scientific knowledge of the late effects of TBI. By building upon existing clinical data collection infrastructure from ongoing longitudinal studies of individuals with TBI, the LETBI study aims to make inferences about possible post-traumatic neurodegenerative pathogenesis in individuals with remote injuries and enable identification of *in vivo* signatures of autopsy-confirmed neuropathology.

The central hypothesis of the LETBI project is that TBI is associated with pathologic abnormalities detectable by neuropathological analyses that correlate with ultra-high resolution *ex vivo* magnetic resonance imaging (MRI) biomarkers, *in vivo* MRI biomarkers, and neurobehavioral phenotypes. We designed the LETBI project's protocols to test this hypothesis, and to facilitate discovery science and hypothesis generation.

Methods

Study design: Overview

Patients are screened for prospective enrollment in the LETBI project based on their participation in ongoing cohort studies led by the investigative team, including the Adult Changes in Thought (ACT) study, the TBI Model Systems (TBIMS), and the TBI-Health study.

The ACT study has been continuously funded by the National Institutes of Health (NIH) since 1994 and includes volunteers from a random sample of community dwelling non-demented Kaiser Permanente Washington (formerly Group Health) members over age 65 who are followed on a 2-year cycle to identify incident dementia cases.⁹ To date, the study has enrolled more than 5400 people, approximately one quarter of whom have signed autopsy consents. ACT data sources include genome-wide single nucleotide polymorphism data, computerized pharmacy, clinical laboratory, and medical record data. At baseline and each study visit, TBI exposure history is queried using standardized methods, and de-

codes of medical records for ACT participants are available to characterize medical care received for TBI.

The TBIMS is funded by the National Institute on Disability, Independent Living and Rehabilitation Research. This prospective study enrolls individuals with complicated mild-to-severe TBI at the time of inpatient rehabilitation, collecting extensive clinical and functional metrics with which to characterize the index TBI, and follows them at 1, 2, and 5 years post-injury and every 5 years thereafter.¹⁰ The LETBI study recruits participants from two TBIMS centers: The Brain Injury Research Center at Mount Sinai (BIRC-MS), first funded in 1987, and the University of Washington (UW) TBIMS, first funded in 1998.

The TBI-Health study in the BIRC-MS was funded by the Centers for Disease Control and Prevention in 2012 and enrolls individuals who are at least 1 year post-hospitalization for TBI. The TBI-Health study gathers uniform metrics and medical record data to characterize the index TBI, and participants are followed biannually to gather neuropsychological data, self-report measures of mood and health, and clinician and caregiver ratings of behavior and function.

Recruitment and eligibility criteria

Individuals in the aforementioned studies are invited to participate in LETBI if they meet at least one of the following inclusion criteria: 1) history of complicated mild, moderate, or severe TBI defined as a blow to the head resulting in at least one of the following: Glasgow Coma Scale score <13 on emergency department admission, loss of consciousness (LOC) >30 min, post-traumatic amnesia >24 h, or trauma-related intracranial abnormality on neuroimaging, or 2) history of two or more mild TBIs defined as an external blow to the head that results in physiological disruption of brain function or altered mental status; LOC if present is <30 min, post-traumatic amnesia if present is <24 h, and Glasgow Coma Scale score \geq 13.¹¹ LETBI enrollment began in 2014 with a goal of recruiting a convenience sample of at least 100 participants. Many survivors of TBI have contraindications to MRI due to implanted hardware and metallic devices, so those who are unable to complete *in vivo* MRI are included in the study to ensure that the LETBI cohort is representative of the population of interest. Only individuals who assent/consent to brain donation are enrolled in the LETBI project. Informed consent to participate in the LETBI project is obtained from the participant, or from his/her surrogate if he/she is unable to provide informed consent. Control brain specimens from individuals with no history of TBI or neurological or psychiatric disease and no abnormalities detected on gross pathological analysis are acquired from patients who come to autopsy through partner studies at LETBI sites (UW, Mount Sinai, Brigham and Women's Hospital and Massachusetts General Hospital [BWH/MGH]), with informed consent provided by the patient or his/her surrogate. Control brains only undergo the *ex vivo* protocols described below.

Neurobehavioral evaluation

An overview of study procedures is shown in Figure 1. All participants undergo a standardized neurobehavioral evaluation, which includes a battery of NIH Common Data Elements (CDEs).¹² Neuropsychological tests measure attention, working memory, processing speed, verbal fluency, and visuo-motor sequencing.

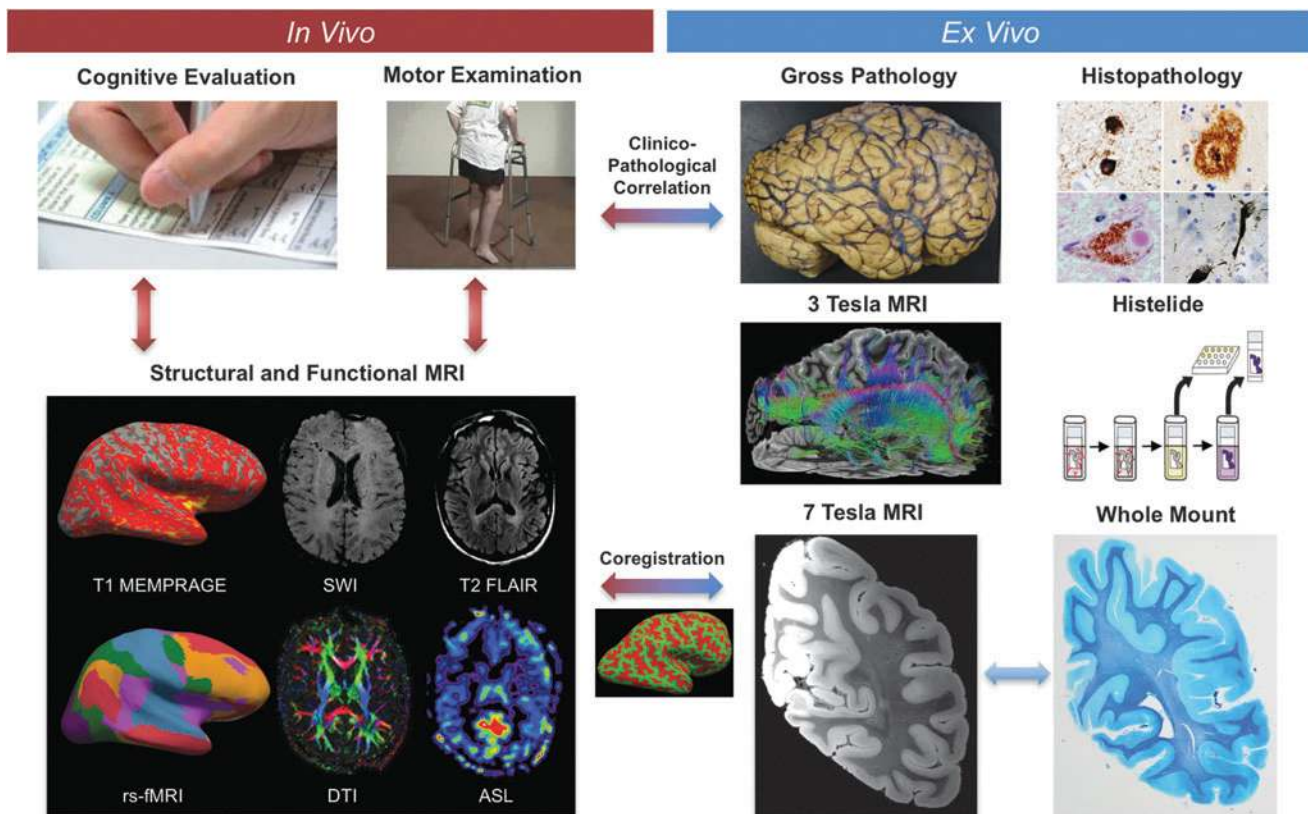


FIG. 1. Overview of study design. The Late Effects of Traumatic Brain Injury (LETBI) study integrates *in vivo* data (left) and *ex vivo* data (right) to comprehensively characterize post-traumatic neurodegeneration. LETBI participants undergo extensive cognitive, behavioral, and neurological examinations. In addition, structural and functional magnetic resonance imaging (MRI) are performed and blood samples are drawn for proteomic and genomic analysis to identify *in vivo* biomarkers of post-traumatic neuropathology. Autopsied brain specimens undergo gross pathological analysis, histopathological analysis including Histelide and whole-mount analysis, and ultra-high resolution *ex vivo* MRI on 3 Tesla and 7 Tesla MRI scanners. Co-registration of *ex vivo* and *in vivo* MRI data enables determination of whether pathologically relevant *ex vivo* lesions were present during life. *In vivo* signatures of postmortem pathology are then correlated with cognitive and behavioral data to characterize the clinical phenotype(s) associated with pathological lesions. Color image is available online at www.liebertpub.com/neu

LETBI investigators assess motor symptoms and functional independence, and patients provide self-reported measures of mood and function. A summary of these assessments is provided in Table 1.

Proteomic and genomic studies

A blood sample is drawn and prepared for proteomic and genomic analysis. Remaining plasma and serum are isolated and banked for future planned studies. Blood processing and storage protocols are harmonized with those of the National Institute of Neurological Disorders and Stroke-funded Transforming Research and Clinical Knowledge in TBI study.¹³

In vivo MRI acquisition

Brain MRI is performed within a week of cognitive and behavioral assessments. Patients at Mount Sinai are scanned using a Siemens Skyra (Siemens Medical Solutions, Erlangen, Germany) 3 Tesla (3T) MRI scanner with a 32-channel head coil for signal reception. Patients at UW are scanned using a Philips Achieva 3T MRI scanner with a 32-channel head coil. To facilitate pooling of MRI data from Mount Sinai and UW, we developed a harmonized protocol of high-resolution structural and functional sequences with only minor variances in the imaging parameters across sites (Supplementary Table 1; see online supplementary material at <http://www.liebertpub.com>). The LETBI *in vivo* MRI protocol in-

cludes T1 multi-echo Magnetization Prepared Rapid Acquisition Gradient Echo (MEMPRAGE) for volumetric analyses,¹⁴ susceptibility weighted imaging for detection of traumatic microhemorrhages,¹⁵ diffusion MRI for tractography-based structural connectivity analysis,^{16,17} and resting state functional MRI for functional connectivity analysis.¹⁸ Sequence selection for LETBI was designed to maximize consistency with the NIH CDEs for TBI Neuroimaging.^{19,20}

In vivo MRI processing and analysis

In vivo MEMPRAGE and diffusion MRI data undergo a series of FreeSurfer-based processing procedures, as previously described.^{14,21} MEMPRAGE data are used to generate cortical and subcortical morphometrics, while diffusion data are used to measure anisotropy and diffusivity in white matter tracts. Resting-state fMRI data are processed using independent component analysis²² and seed-based analysis to measure functional network connectivity.²³

Each *in vivo* dataset is also assessed for pathoanatomic lesions, which are classified using the NIH CDEs for TBI Neuroimaging²⁴ and if applicable, NIH CDEs for Stroke Neuroimaging.²⁵ These classification systems are similarly applied during the *ex vivo* MRI lesion analysis, allowing correlation of the *in vivo* and *ex vivo* lesion data. Importantly, a second analysis of the *in vivo* MRI data is performed for participants who come to autopsy and undergo *ex vivo* MRI. The *ex vivo* MRI data are co-registered to the *in vivo*

TABLE 1. LETBI NEUROBEHAVIORAL ASSESSMENT PROTOCOL BY DOMAIN

<i>Neurocognitive/behavioral domain</i>	<i>Neurocognitive/behavioral test</i>
Attention/working memory	Wechsler Adult Intelligence Scale-4th Edition (WAIS-IV) Digit Span ⁵²
Visuomotor sequencing/processing speed	WAIS-IV Symbol Search & Coding ⁵² Trail Making Test - Trails A & B ⁵⁵
Learning and memory	California Verbal Learning Test-2nd Edition (CVLT-II) ^{54,55} Wechsler Memory Scale-4th Edition (WMS-IV) Logical Memory I & II ⁵⁶ Rey Complex Figure Test (RCFT) ⁵⁷
Verbal fluency	Animal Naming ⁵⁸ Controlled Oral Word Association Test (COWAT) ⁵⁸
Mood/function	Patient-Reported Outcomes Measurement Information System (PROMIS) NeuroQOL Short Forms-Anxiety, Depression, Fatigue, Social Participation ⁵⁹
Psychosocial problems	Law/Violence/Psychiatric Hospitalization/Suicide Attempt- three items from TBIMS ⁶⁰
Life satisfaction	Satisfaction With Life Scale (SWLS) ⁶¹
ADLs	RAND Short Form 36-Item Health Survey (SF-36) ⁶²⁻⁶⁴
Motor signs	Uniform Parkinson's Disease Rating Scale (UPDRS) Motor Exam ⁶⁵
Impulsivity and aggression	Personal Evaluation-Barratt Impulsivity Scale II ⁶⁶ Brown-Goodwin Lifetime History of Aggression ⁶⁷
Demographics	TBI Common Data Elements - Demographic & Socioeconomic Status ⁶⁸
Self-reported medical conditions	List of medical conditions adapted from the ACT Study ⁸
Self-rated health	Health rating adapted from the Midlife in the United States (MIDUS) Study ⁶⁹
TBI history	Brain Injury Screening Questionnaire (BISQ) Part 1 ^{70,71}
Physical performance	Short Physical Performance Battery ⁷²
Alcohol/substance use	Alcohol, Smoking, and Substance Involvement Screening Test (ASSIST) ^{73,74}

LETBI, Late Effects of Traumatic Brain Injury study.

MRI data (see below), providing an opportunity to assess the *in vivo* MRI signal properties at the precise spatial coordinates where the *ex vivo* MRI lesions are identified. Specifically, the *ex vivo* MRI data are used to identify lesions that escaped detection during the initial review of *in vivo* MRI data.

Longitudinal follow-up

All participants in the LETBI project agree to brain donation, and participants are encouraged to discuss their wishes with family members and significant others. The study team provides participants and their families with information about brain donation, in addition to detailed instructions to follow in the event of death. The study team contacts participants every 6–9 months via telephone and sends holiday and birthday cards to maintain updated contact information.

Verbal autopsy

Participants in the LETBI study are asked to provide contact information for at least two informants who know them well and who may be willing to participate in an interview in the event of death of the participant. The purpose of this postmortem interview is to gather information about the participant's cognitive, motor, emotional, and medical health in the year(s) prior to death. This information supplements data gathered through study visits and medical record review, including TBI exposure as ascertained by the Brain Injury Screening Questionnaire.²⁶

Brain specimen acquisition and neuropathological protocol

For specimens obtained at UW, a prosector obtains the brain specimen and a rapid autopsy, consisting of dissection of one hemisphere for ~60 flash frozen specimens, is performed in cases with postmortem interval (PMI) <8 h. The remaining portion of the dissected hemisphere (or one intact hemisphere in non-rapid autopsies) is fixed in 10% formalin prior to undergoing comprehensive sampling and analysis for pathologic changes of AD, Lewy

body disease, vascular disease, TBI, hippocampal sclerosis, frontotemporal lobar degeneration, and others according to ACT protocols aligned with the latest diagnostic guidelines.²⁷⁻³¹ In selected fixed tissues, Histelide analysis is performed for quantitative, molecularly specific analyses of pathologic peptides including phospho-tau species (see below).^{32,33} The contralateral hemisphere from every case is fixed in 10% formalin and sent to BWH/MGH for gross pathological analysis and further fixation. For specimens obtained at Mount Sinai, whole brains are fixed in 10% formalin and sent to BWH/MGH for *ex vivo* MRI. To ensure adequate fixation and to prevent specimen flattening (which can prevent specimens from fitting into custom *ex vivo* MRI coils and can distort the MRI data), we implemented a series of standard procedures for optimal brain fixation and specimen processing, as detailed in the Supplementary Material.

Histopathological analysis: Histelide

The steps involved in Histelide analysis are detailed elsewhere^{32,33} and in the Supplementary Material Methods.

Ex vivo MRI acquisition

Ex vivo MRI is performed on selected autopsy brain specimens that meet the following *a priori* selection criteria: 1) postmortem fixation interval (time from death to fixation of the specimen) <48 h; 2) availability of comprehensive, prospectively acquired cognitive and behavioral data; and 3) availability of *in vivo* MRI data acquired prospectively with the LETBI protocol. Each *ex vivo* MRI sequence was designed to provide complementary information about post-traumatic dementia pathology and to create opportunities to identify novel MRI biomarkers. Each *ex vivo* MRI sequence also provides unique tissue contrast and signal characteristics that correspond to those of an *in vivo* MRI sequence, as shown in Supplementary Table 2.

Brain specimens are first scanned on a 7T Siemens Magnetom MRI scanner using a custom-built head coil. The design, technical specifications, and signal-to-noise-ratio evaluations of the coil are

detailed in the Supplementary Material Methods. For the 7T scan, we utilized a multi-echo FLASH (MEF) sequence³⁴ at 200 μm spatial resolution. Total scan time on the 7T MRI scanner is 18 h and 31 min. Next, specimens are scanned on a 3T Siemens Tim Trio MRI scanner for 41 h and 45 min using a 32-channel head coil. MEF data are also collected at 3T at 1 mm spatial resolution for generating surface reconstructions. Diffusion data are acquired using a 3D diffusion-weighted steady-state free-precession sequence³⁵ at 750 μm spatial resolution. Total diffusion scan time is 30 h and 31 min. Parameters for all 7T and 3T *ex vivo* sequences are detailed in Supplementary Table 3.

Ex vivo MRI processing and analysis

MEF data acquired on the 7T and 3T MRI scanners undergo a series of processing steps, including creation of parameter maps. Parameter maps include proton density and T1 and T2* decay times. These are estimated directly from the MEF acquisitions using the DESPOT1 algorithm^{34,36} to quantify the tissue properties independent of the scanner and sequence types. We use our surface-based registration and segmentation tool FreeSurfer^{37,38} to reconstruct models of the gray/white and pial surfaces for morphometric analysis of the 3T MEF data. Upon completion of data processing, each 7T and 3T MEF dataset is assessed for data quality based upon a visual assessment of anatomic landmarks. If the data are deemed to be of sufficient quality, the MEF datasets are then analyzed by LETBI investigators for pathoanatomic lesions in two phases.

In the first phase of *ex vivo* MRI data analysis, the 7T and 3T MEF datasets are assessed for pathoanatomic lesions that can be classified using the NIH CDE Guidelines for TBI and Stroke Neuroimaging.^{19,25} In the second phase, we assess for pathoanatomic lesions that are not currently accounted for by the NIH CDE criteria, which were generated for *in vivo* MRI lesion characterization. In this second phase, lesions identified on the 7T and 3T MEF datasets are classified based upon their signal characteristics, neuroanatomic location, and morphology.

Diffusion data acquired on the 3T MRI scanner are processed for deterministic tract construction using Diffusion Toolkit and analyzed for connectivity using TrackVis (www.trackvis.org), as previously described.³⁹ All major association, projection, and commissural white matter bundles in the cerebral hemispheres are analyzed for structural connectivity using the region of interest (ROI) approach described in Catani and de Schotten's tractography atlas.⁴⁰ In addition to the white matter bundles described in this atlas, thalamo-cortical tracts are identified using a single-ROI approach⁴¹ and brainstem arousal pathways are identified using a multi-ROI approach.^{42,43} All tract bundles are inspected for hemispheric asymmetry and/or focal disruptions, compared with a cohort of control brain specimens from patients who died of non-neurological diseases and had no known history of trauma. In addition, any lesion identified during the *ex vivo* MRI lesion analysis is used as a seed for the generation of fiber tracts. Using this seed-based lesional approach, the pathophysiological impact of each lesion on its associated white matter pathways is defined. *Ex vivo* MRI acquisition and processing methods are identical for control and TBI specimens.

In summary, the *ex vivo* MRI analyses provide four sets of data that are subsequently correlated with histopathological and *in vivo* MRI data: 1) NIH CDE-based lesion analysis of 7T and 3T MEF data; 2) analysis of lesions detected by 7T and 3T MEF data that are not currently accounted for by the NIH CDEs; 3) 3T diffusion tractography analysis of white matter disruption via screening of all major white matter bundles; and 4) 3T diffusion tractography analysis of white matter disruption related to focal lesions.

Co-registration of in vivo and ex vivo MRI data

We used the combined volume- and surface-based registration (CVS) framework⁴⁴ to spatially register the corresponding *in vivo*

and *ex vivo* MRI datasets. CVS is a pair-wise registration method that has been shown to optimize the alignment of both cortical and subcortical areas in brain volumetric MRI. Additional details are provided in the Supplementary Material Methods.

MRI-guided brain cutting, imaging-pathology procedures, whole-mount immunohistopathology

Following *ex vivo* MRI of fixed hemibrain and whole brain specimens, ACT brains are shipped from MGH/BWH to the UW Neuropathology and Targeted Molecular Testing Core, and TBIMS/TBI-Health brains are shipped to the Brain Tissue Repository and Neuropathology Core of the Center for Neuroscience and Regenerative Medicine, at Uniformed Services University of the Health Sciences in Bethesda, MD.⁴⁵ Slabs are selected at both institutions (see below) for whole-mount sectioning, neuropathologic assessment using routine morphologic stains, immunohistochemistry, histochemistry for myelin and iron, and image digitalization of the resultant slides. Each specimen is sectioned into three parts: the cerebral hemisphere(s), brainstem, and cerebellum. The hemisphere specimens are sectioned coronally and photographed to obtain an overview of brain structures within hemisphere(s) in both projections: rostral (frontal) and caudal (occipital). Slabs are then selected for whole-mount analysis during a consensus video teleconference in which the neuropathology team and imaging team compare cortical and subcortical anatomic landmarks on the coronal slabs with corresponding landmarks on the *ex vivo* MRI datasets. Based on this landmark comparison, the precise neuroanatomic coordinates of each lesion identified on *ex vivo* MRI is used to guide the selection of the corresponding coronal slab.

Coronal slabs are embedded in oversized paraffin blocks and serially sectioned at 50 μm thickness. For ACT cases, unselected slabs undergo routine neuropathological analysis to maintain continuity of neuropathological data for the ACT study. For slabs selected for whole-mount analysis, the level of sectioning within each block is guided by identification of lesions on *ex vivo* MRI acquisition. With an interval of 200 sections (1 cm), we cut 10 serial sections at 10 microns thick to be stained for hematoxylin and eosin (H/E), Luxol-fast Blue (LFB), Perls' stain (iron), hyperphosphorylated-tau (pTau; AT8), phosphorylated α -synuclein (p α -syn), amyloid precursor protein (APP), 1–42 β -amyloid (4G8), phosphorylated-TAR DNA-binding protein 43 (pTDP-43), glial fibrillary acidic protein (GFAP), and activated microglia (CD68 and iba-1). When indicated, we obtain ~ 20 levels through the entire hemisphere to survey the full distribution of pathology. The separated brainstem specimen is sectioned in the axial plane to obtain four tissue blocks. Each block is then embedded, serially sectioned and stained as described previously⁴² or saved for future analyses. The cerebellum is saved for future analysis.

Consensus conferences for validation of neuropathology and imaging biomarkers

We use VS NIS-SQL software to allow real-time on-line simultaneous viewing of scanned whole-mount slides at each study site. Conference goals are to correlate neuropathological findings with study records, clinical data, *in vivo* MRI and *ex vivo* MRI. Digitized slides are also viewed and discussed in this forum. This is an opportunity to regularly assemble an expert panel to consider histopathologic and other end-points to achieve meaningful associations and identify effective diagnostic approaches.

Results

Enrollment summary

As of September 2017, 158 individuals with TBI have enrolled in the LETBI study, all of whom consented to brain donation. A

subsample of 105 participants completed *in vivo* MRI. Those with contraindications to MRI, including implanted devices that were MRI incompatible, were excluded. Those with claustrophobia or MRI-safe devices that caused substantial artifact did not complete the MRI scan. Thus far, eight individuals have come to autopsy. All eight brains have been successfully acquired by the LETBI study team, and to date six have undergone *ex vivo* MRI; data analysis and interpretation are ongoing.

Index case: Demographic and clinical data

Here, we use data collected from the first participant to complete the *ex vivo* LETBI protocol to illustrate the LETBI study methods and data integration protocols. This individual is a right-handed female with a high school education who lived independently in a senior apartment until death around age 90. She enrolled in the ACT study in her late 60s, reporting no chronic medical conditions, but her history was notable for TBI. Her lifetime exposure to TBI is summarized in Table 2.

Cognitive and functional data

Our index case completed the LETBI neurobehavioral protocol in her mid-80s (after her first two TBIs, which occurred >60 years and 4 years prior, respectively). She performed well on this comprehensive battery of cognitive tests. Based on this evaluation, she was given the clinical diagnosis “normal cognition.” On the Uniform Parkinson’s Disease Rating Scale motor examination, her right leg agility could not be assessed, her ability to rise from a chair was “slow, or may need more than one attempt,” her posture was “not quite erect, slightly stooped” and her gait was normal but notable for “retropulsion, but recovers unaided.” She reported no neurobehavioral or mood symptoms and reported no difficulties on the Functional Assessment Questionnaire.

The patient participated in ACT study visits every 2 years from her late 60s to death (11 visits total). She described her health as “good” or “very good” at all ACT study visits. She was consistently overweight (body mass index = 25–30) and was diagnosed with hypertension and sleep apnea in her early 80s. Her *APOE* genotype was $\epsilon 2/\epsilon 3$, and she reported no family history of dementia. She consistently reported exercising at least 15 min every day, until her last study visit when she indicated her exercise was reduced to 4 days per week. She reported no difficulty with activities of daily living including bathing, dressing, feeding, toileting, or walking until age 83 when she had “some difficulty” getting out of a bed or a chair, and by age 89 reported “a lot of difficulty” with these

activities. Her balance was not assessed at her last study visit, but at age 87 she was only able to perform a semi-tandem (as opposed to full tandem) walk.

In vivo MRI: NIH Common Data Elements assessment

3T MRI was performed at age 88, after her fifth TBI. The T2 fluid-attenuated inversion recovery sequence revealed two pathoanatomic lesions: lesion 1, punctate hyperintensities in the corona radiatae and internal capsules of both hemispheres (Fig. 2 and Supplementary Fig. 1); and lesion 2, bilateral periventricular hyperintensities (Supplementary Fig. 1; Supplementary Table 4). These lesions were classified using the NIH Common Data Elements for TBI Neuroimaging and Stroke Neuroimaging as being consistent with leukoaraiosis or possibly chronic traumatic axonal injury (Supplementary Table 4).

Cause of death

Following her sixth documented TBI (Table 2), a head computed tomography scan demonstrated a right parietal subdural hemorrhage with subfalcine herniation and 1.1 cm of right-to-left midline shift at the level of the septum pellucidum. She underwent craniotomy for evacuation of the subdural hemorrhage and recovered well over the following week. She was transferred to a subacute nursing facility for rehabilitation, but she then experienced an episode of high blood pressure, slurred speech, and facial drooping, for which she was readmitted to hospital. She experienced several similar episodes while in the hospital, as well as episodes of expressive aphasia and delirium. No definitive etiology of these transient events was determined despite diagnostic evaluation. Her clinical condition deteriorated, necessitating surgical placement of a percutaneous gastric tube, which was contrary to her previously documented wishes. She was therefore transferred to hospice care and died approximately 1 month after her injury.

Gross pathological analysis

At autopsy, the patient’s brain weighed 1280 g (unfixed) and postmortem interval to brain fixation was 4 h. There was no evidence of mass lesions, destructive lesions, or herniation. There was mild cortical atrophy involving the frontal, temporal, and parietal lobes; occipital lobes were relatively spared. Surface analysis of the gross, unfixed brain specimen revealed golden discoloration of the right inferior frontal gyrus and superior temporal gyrus, suggesting hemosiderin deposition from previous subarachnoid hemorrhage (Supplementary Fig. 2). Gross examination for other focal lesions

TABLE 2. TIMELINE OF TRAUMATIC BRAIN INJURIES FOR INDEX PATIENT

TBI #	Age	Mechanism of injury	Severity of injury	Reporting source
1	Mid 20s	Head-on MVA without seatbelt restraints	LOC at least 1 min	Self-report at ACT study entry
2	Early 80s	MVA resulting in deployed airbags; destroyed both vehicles	LOC several minutes	Self-report, medical records, other report (adult child who completed postmortem interview)
3	Late 80s	Fall	Unknown	
4		Fall	Unknown	
5		Fall	Unknown, required hospitalization	
6		Fall	Head CT revealed subdural hemorrhage and midline shift	

TBI, traumatic brain injury; MVA, motor vehicle accident; LOC, loss of consciousness; ACT, Adult Changes in Thought study; CT, computed tomography.

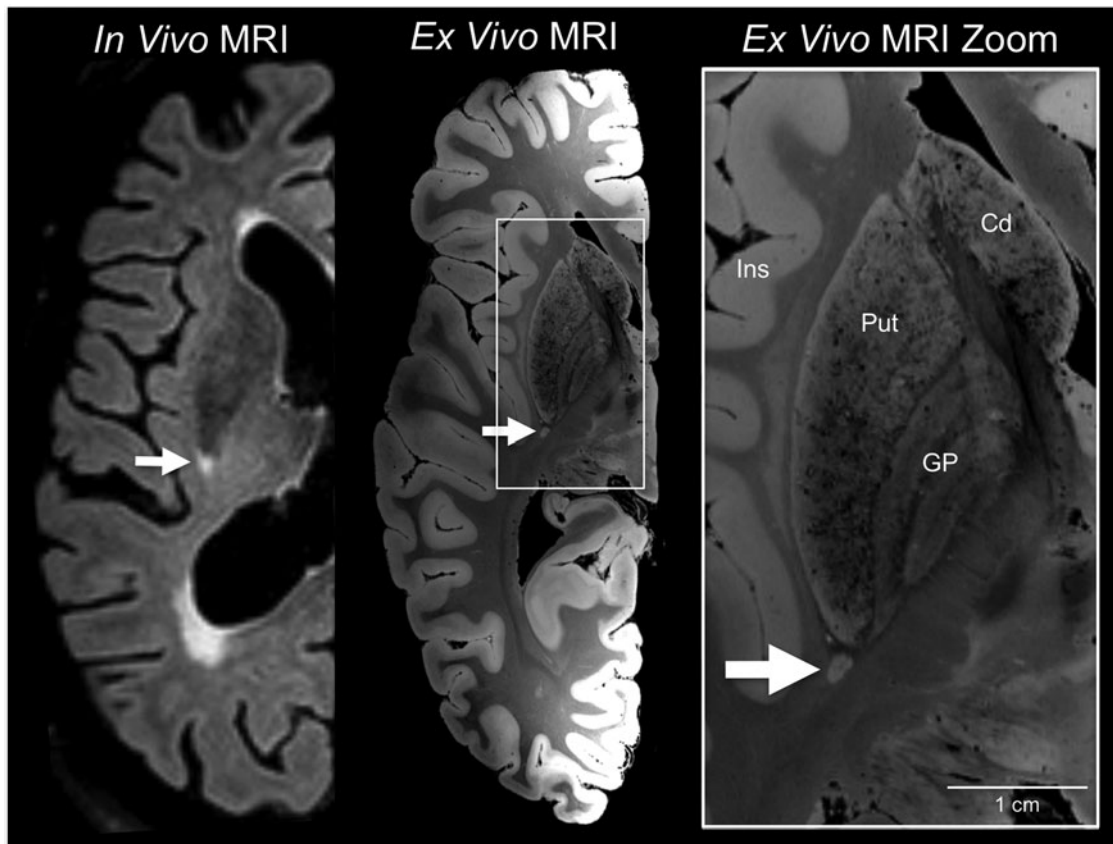


FIG. 2. White matter lesion identification on *in vivo* 3 Tesla magnetic resonance imaging (MRI) and *ex vivo* 7 Tesla MRI. An *in vivo* 3 Tesla MRI performed at age 88, after the patient's fifth TBI, revealed bihemispheric corona radiata and internal capsule white matter hyperintensities, including a punctate lesion at the posterior aspect of the putamen (arrow). The same lesion was identified by *ex vivo* 7 Tesla MRI (arrow), which was performed on the formalin-fixed right hemisphere. A zoomed view of the lesion is shown in the right panel (arrow) to demonstrate the increased anatomic precision provided by *ex vivo* MRI (200 μm resolution) for delineating the borders of the lesion with respect to nearby anatomic structures. Cd, caudate; GP, globus pallidus; Ins, insula; Put, putamen.

was negative in the sliced brain (after *ex vivo* imaging studies were completed).

Ex vivo 7T MRI

7T MRI quality assessment revealed excellent delineation of anatomic landmarks (Supplementary Fig. 3) and minimal distortions related to air bubbles. In the first phase of *ex vivo* MRI lesion analysis, we observed the same two lesions seen on *in vivo* MRI: punctate hyperintensities in the corona radiata and internal capsule (lesion 1; Fig. 2) and periventricular hyperintensities – (lesion 2; Fig. 3 and Fig. 4A). A summary of the NIH Common Data Element analysis for *ex vivo* MRI is provided in Supplementary Table 5. During the second phase of *ex vivo* MRI lesion analysis, we identified a third and fourth abnormality. Lesion 3 was a curvilinear lesion that followed the outline of the superficial cortex in the frontal operculum (Fig. 3 and Fig. 5). Lesion 4 was a focal, well-circumscribed lesion in the occipital white matter, posterolateral to the occipital horn of the lateral ventricle (Fig. 3).

Ex vivo 3T MRI

Tractography analysis of the major association, projection, and commissural white matter bundles revealed a fifth lesion:

a focal decrease in the relative density of reconstructed fiber tracts in the parietal region of the corpus callosum. Lesion 5 is best illustrated when compared with the corresponding region of fiber tracts in a control dataset from a 60-year-old woman who died of non-neurological causes (Fig. 6). The density of fiber tracts visualized in other white matter bundles, such as the corticospinal tract and cingulum bundle, was similar to those of the control dataset (Supplementary Fig. 4 and Supplementary Fig. 5), indicating that the callosal tract abnormality did not represent global tract loss. The lesion-based tractography analysis revealed that lesion 4 caused minimal tract disruption within the inferior longitudinal fasciculus and the inferior fronto-occipital fasciculus (Supplementary Fig. 6), which is consistent with the patient's high-level performance on tests of associated cognitive functions such as memory and attention.

Integration of *ex vivo* MRI and *in vivo* MRI

CVS-based co-registration was performed to align the *ex vivo* 7T MEF and *in vivo* 3T T1 MEMPRAGE datasets (Fig. 7). Once anatomic alignment was confirmed, the precise anatomic coordinates of the occipital lesion, as detected on the *ex vivo* 7T MEF dataset, were identified on the *in vivo* 3T T1 MEMPRAGE dataset. At these

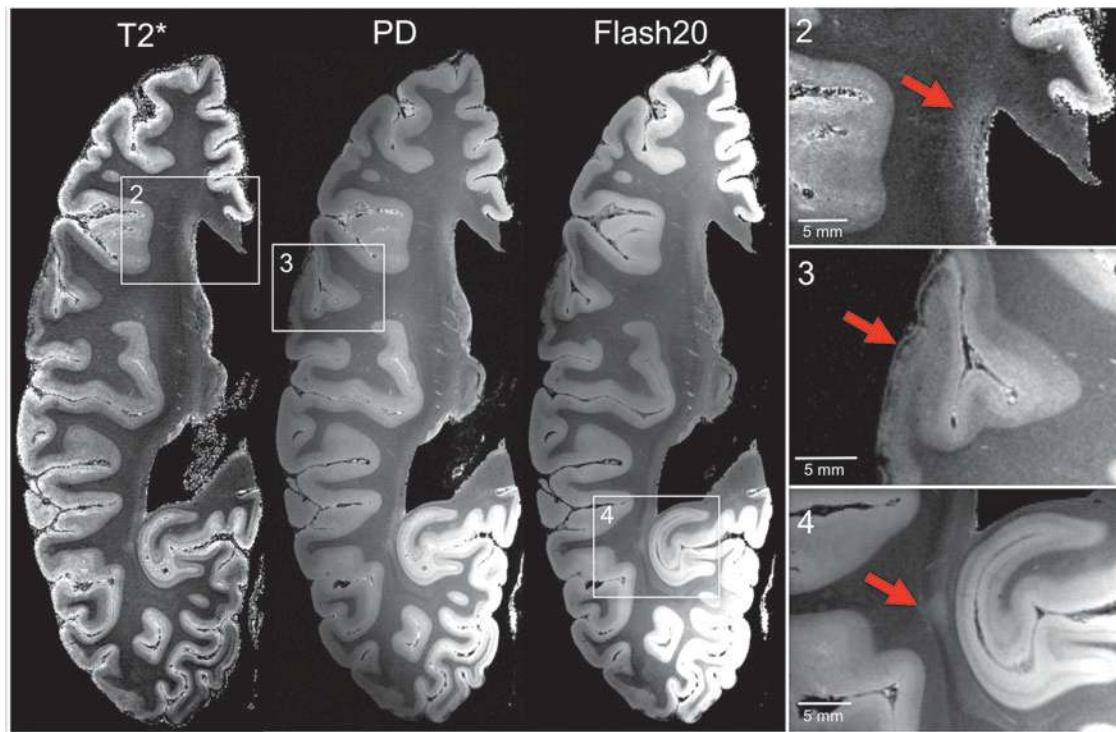


FIG. 3. *Ex vivo* 7 Tesla magnetic resonance imaging (MRI) reveals focal lesions not detected by *in vivo* 3 Tesla MRI. Axial T2*, proton density (PD), and flash20 images synthesized from the multi-echo flash sequence are shown at the level of the superior border of the thalamus. These three datasets reveal two lesions that were not visualized on the *in vivo* MRI dataset (lesions 3 and 4) and confirm the presence of a lesion that was seen *in vivo* (lesion 2). Lesion 2 is a periventricular hyperintensity in the frontal lobe, suggesting leukoaraiosis. Lesion 3 is a curvilinear hypointensity that traverses the superficial layers of cerebral cortex in the frontal operculum, suggesting hemosiderin deposition. Lesion 4 is a punctate hyperintensity in the periventricular white matter of the occipital lobe, consistent with leukoaraiosis or possibly chronic traumatic axonal injury. Zoomed views of each lesion are shown on the inset panels, with red arrows indicating the lesions. Color image is available online at www.liebertpub.com/neu

coordinates, a hypointense focus was observed on the *in vivo* 3T T1 MEMPRAGE dataset taken after her 5th TBI, 2 years prior to death (Fig. 8). Notably, this hypointense focus was not identified as a lesion during the *in vivo* CDE analysis performed by our research team.

Histopathological analysis

Standard histopathological analyses, performed blind to MRI findings, revealed phospho-tau immunoreactive neurofibrillary tangles in pre-alpha cells of the transentorhinal cortex, CA1 sector of hippocampus, and subiculum, but absent in other sectors of hippocampus, entorhinal cortex, isocortex, primary sensory cortex, or granule neurons of dentate fascia (Braak stage III). A β neuritic or diffuse plaques as determined by Bielschowsky and A β immunostains (4G8) were absent in neocortex, isocortex, hippocampus, striatum, midbrain, and cerebellum indicating a Thal phase 0 of 5 for β -amyloid distribution.⁴⁶ Cerebral amyloid angiopathy was absent. Cortical Lewy bodies were evaluated by H/E stain and by α -synuclein immunohistochemistry and were absent in all regions examined. Moderate arteriolosclerosis was present in sections of neocortex and deep gray matter. Microvascular brain injury was absent, and chronic infarcts were not identified. Hippocampal sclerosis was not identified, and phospho-TDP-43 pathology was absent in hippocampus and in the entorhinal/medial temporal cortex. Together, these findings suggest no evidence of pathological processes of AD, Lewy body disease, fronto-

temporal dementia, or vascular brain injury. The presence of neurofibrillary tangles in the hippocampus in the absence of β -amyloid pathology indicates definite primary age-related tauopathy, which often is seen in the absence of clinical dementia or mild cognitive impairment.⁴⁷

In the MRI-guided histopathological analysis, focal lesions identified on *in vivo* and *ex vivo* MRI were evaluated for their histopathological correlates. Within the periventricular white matter lesion (lesion 2), histopathological analysis revealed moderate numbers of granular to linear APP-immunoreactive axonal profiles adjacent to a medium-sized parenchymal vessel (Fig. 4C). The degree to which chronic microvascular disease versus chronic traumatic axonal injury contributed to the pathogenesis of this axonal pathology cannot be definitively determined, but the periventricular and perivascular location is consistent with a vascular etiology. For the curvilinear cortical lesion (Fig. 3; lesion 3), histopathological analysis revealed cortical gliosis associated with numerous hemosiderin-containing microglia (Perls' positive) and neuronal loss consistent with a healed contusion (Fig. 5). In addition, histopathological examination of nearby cortex in the frontal operculum revealed phospho-tau deposition, as well as APP-immunoreactive axons in the underlying white matter (Supplementary Fig. 7).

Whole-mount analysis

For this case, we selected a slab for whole-mount analysis based upon its correspondence with the coronal region that contained lesion

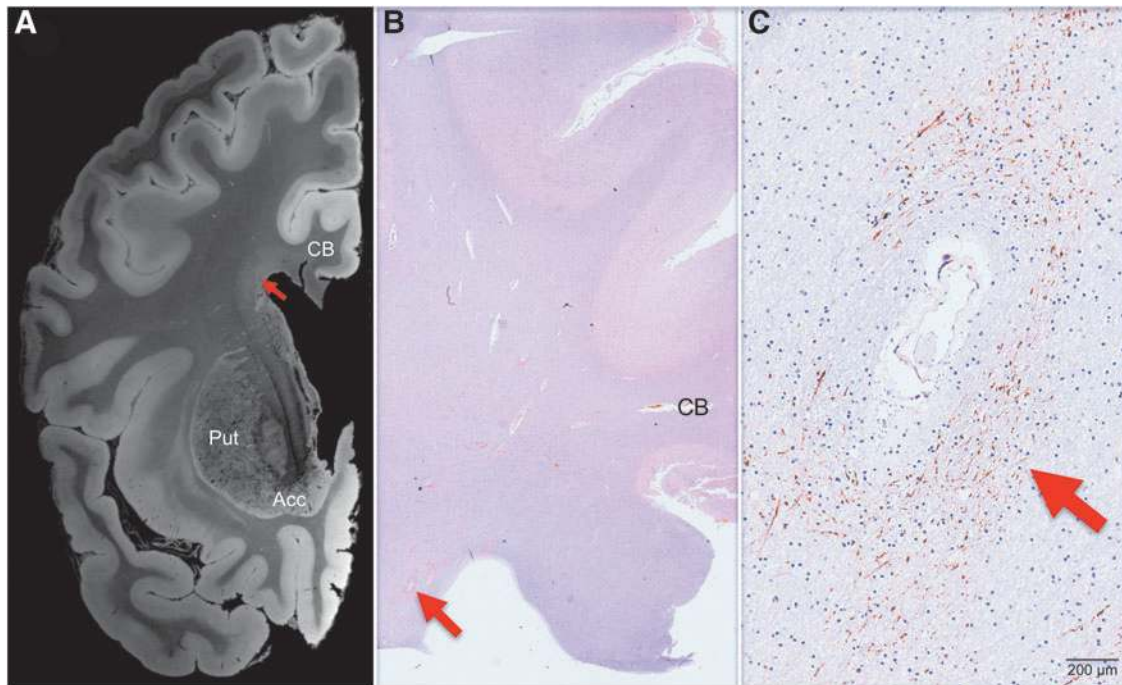


FIG. 4. Correlative analysis of 7 Tesla *ex vivo* magnetic resonance imaging (MRI) and histopathology for the periventricular lesion. (A) A 7 Tesla *ex vivo* MRI coronal image of periventricular signal abnormality (red arrow) is shown at the level of the nucleus accumbens (Acc). The image shown here is a flash20 synthesized image from a multi-echo flash sequence. (B) A coronal histopathological section at the same neuroanatomic location is shown (red arrow), stained with amyloid-precursor protein and counterstained with hematoxylin. (C) Microscopic analysis of the periventricular region revealed disrupted axonal transport, as evidenced by positive amyloid precursor protein staining (red arrow). The degree to which chronic microvascular disease and chronic traumatic axonal injury contributed to this axonal pathology cannot be definitively determined, but the perivascular location suggests a vascular etiology. Neuroanatomic landmarks: CB, cingulum bundle; Put, putamen. Color image is available online at www.liebertpub.com/neu

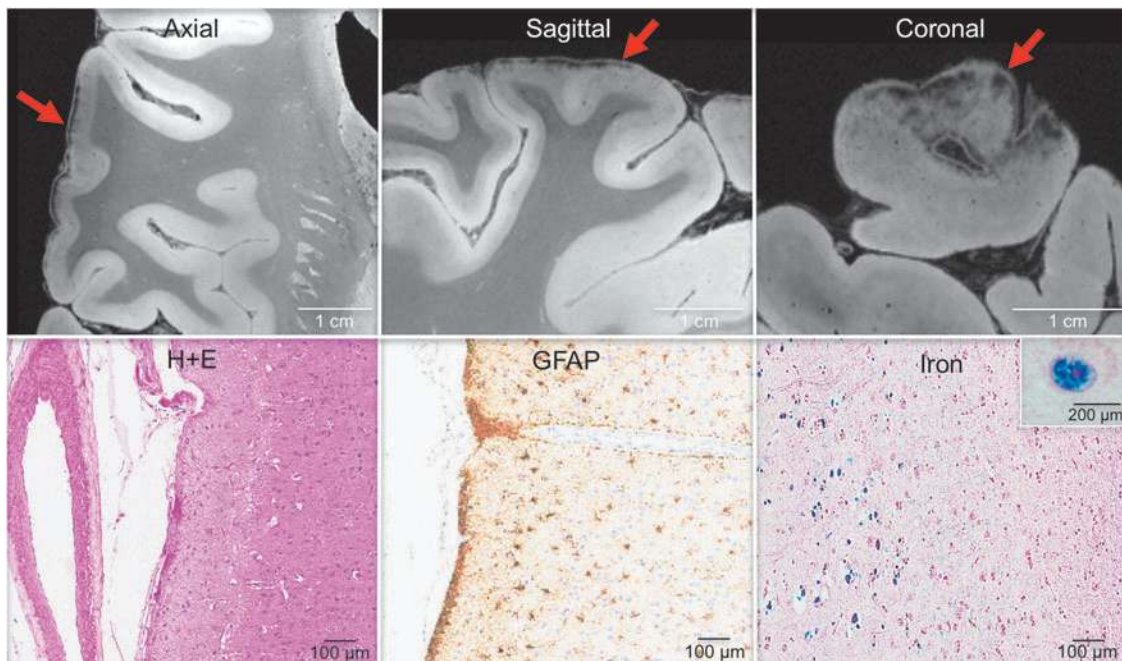


FIG. 5. Correlative analysis of 7 Tesla *ex vivo* magnetic resonance imaging (MRI) and histopathology for the curvilinear cortical lesion. Zoomed views of axial, sagittal and coronal flash20 images synthesized from the 7 Tesla multi-echo flash sequence reveal a curvilinear hypointense signal abnormality (red arrows) in the subpial region of the frontal operculum. Hematoxylin and eosin (H+E) staining of this region revealed atherosclerosis of a vessel within the subarachnoid space. Staining with glial fibrillary acidic protein (GFAP) and Perls' iron stain revealed gliosis and hemosiderin deposition, respectively, in the underlying cerebral cortex. The inset in the bottom right panel shows a high-powered view of hemosiderin-containing microglia. These findings suggest the possibility that a healed contusion accounts for the signal abnormality seen on *ex vivo* MRI. Color image is available online at www.liebertpub.com/neu

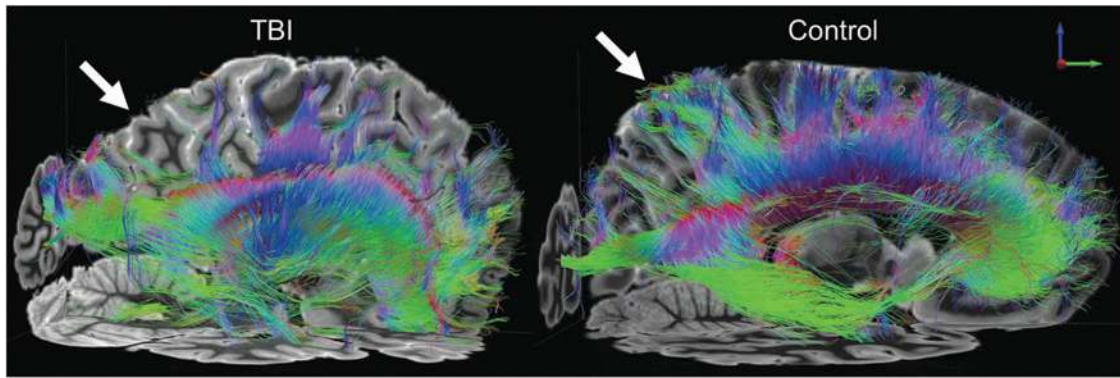


FIG. 6. *Ex vivo* 3 Tesla diffusion tractography reveals regional white matter injury. Transcallosal fiber tracts generated using a corpus callosum seed region are shown from a left lateral perspective for the index patient (left) and a representative control subject who died of non-neurological causes (right). Tractography analysis revealed a decrease in the relative density of transcallosal fiber tracts in the parietal region, compared with the corresponding region of fiber tracts in the control dataset (white arrows). Fiber tracts are color-coded according to their direction (top right inset). Color image is available online at www.liebertpub.com/neu

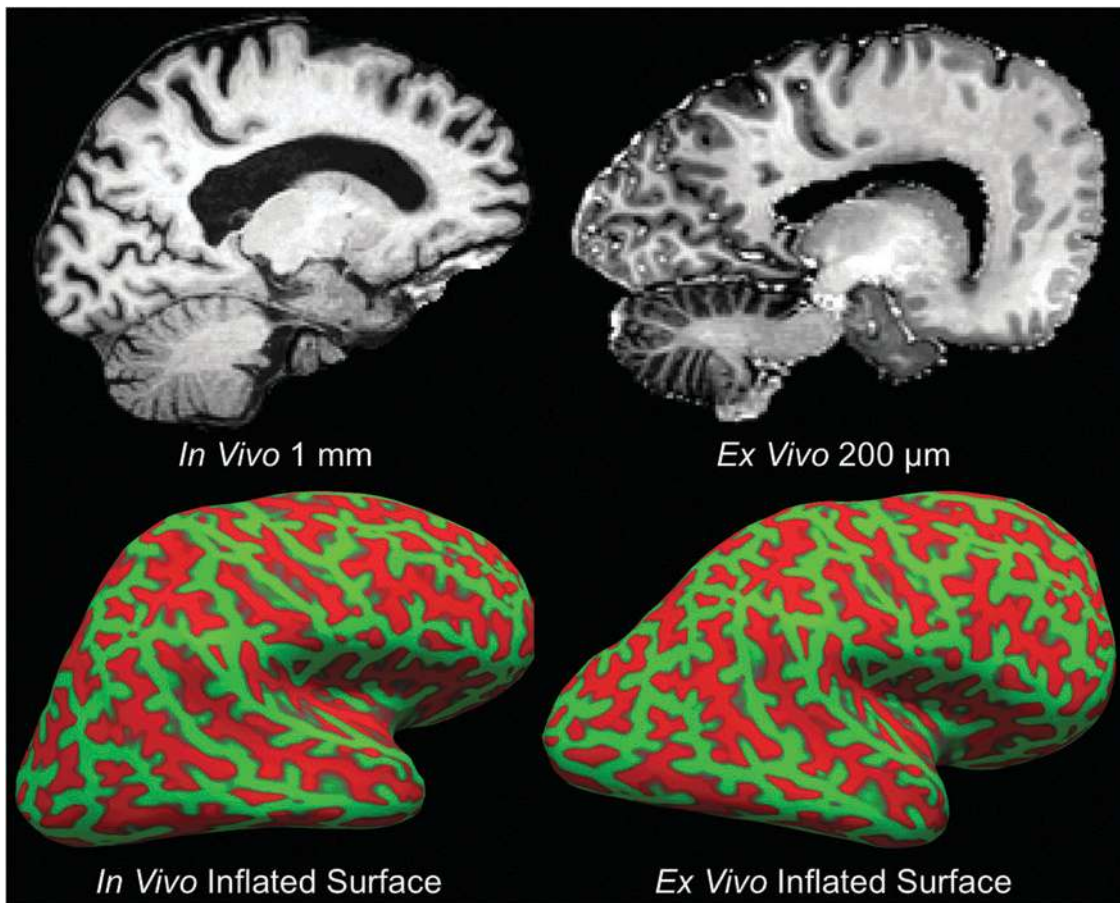


FIG. 7. Co-registration of *ex vivo* and *in vivo* magnetic resonance imaging (MRI) data. Precise anatomic alignment of *in vivo* and *ex vivo* MRI datasets from an individual patient is challenging because postmortem fixation causes nonlinear deformations. A deformation is seen by comparing a sagittal image from the *in vivo* T1 multi-echo Magnetization Prepared Rapid Acquisition Gradient Echo dataset (top left) with a sagittal image from the *ex vivo* multi-echo flash dataset (top right). We developed a combined volume- and surface-based co-registration technique to address this challenge and obtain precise voxel-to-voxel match between the *in vivo* and *ex vivo* datasets. The inflated cortical surfaces generated from the *in vivo* and *ex vivo* datasets are shown in the bottom left and bottom right panels, respectively. Given that the topology of the cortical folds is invariant, this topology can be used to initialize a biomechanical nonlinear deformation. Color image is available online at www.liebertpub.com/neu

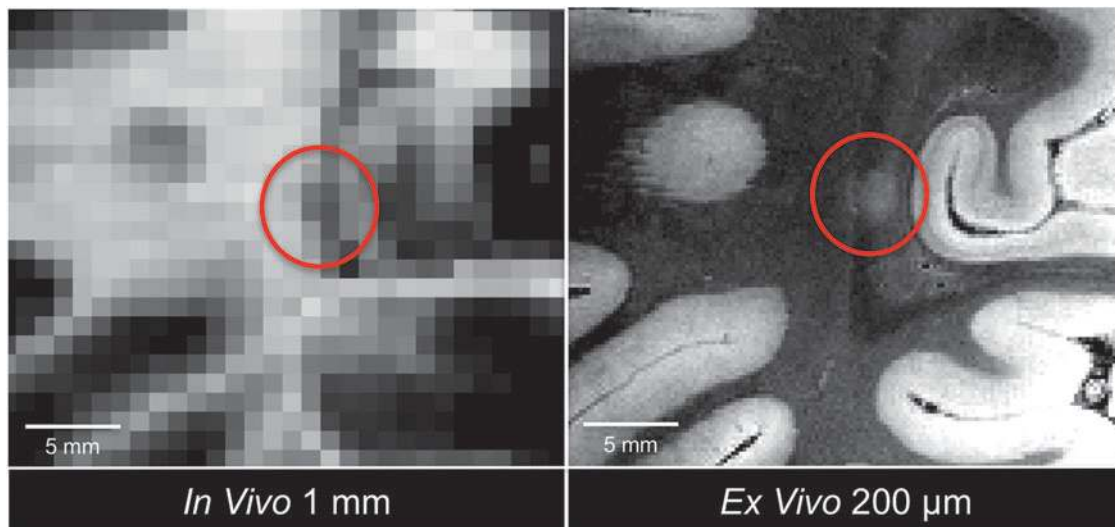


FIG. 8. Co-registration-based lesion localization on *in vivo* magnetic resonance imaging (MRI). Using combined volume- and surface-based co-registration (as shown in Fig. 7), the punctate hyperintense lesion seen in the occipital white matter on the *ex vivo* MRI dataset (red circle, right panel) is colocalized to its precise anatomic coordinates in the *in vivo* MRI dataset (red circle, left panel). The *ex vivo* MRI dataset used in the co-registration was the flash20 parameter map synthesized from the multi-echo flash 7 Tesla acquisition (200 μm spatial resolution), and the *in vivo* dataset was the T1 multi-echo Magnetization Prepared Rapid Acquisition Gradient Echo dataset (1 mm spatial resolution). Although no lesion was detected in the occipital white matter during the initial review of the *in vivo* MRI dataset, there appears to be a punctate hypointensity on the *in vivo* MRI dataset (red circle, left panel) that was only appreciated after the co-registration procedure. This observation suggests that *ex vivo* MRI may reveal lesions that were initially undetected on *in vivo* MRI. Color image is available online at www.liebertpub.com/neu

4 (Fig. 9). Whole-mount analysis using H/E, Perls' iron and LFB/cresyl violet myelin stains revealed neuroanatomical features directly comparable to those seen in the *ex vivo* MRI dataset. Specifically, histopathological analysis revealed enlarged perivascular spaces, corpora amylacea, and white matter rarefaction (Fig. 9D), all of which are likely attributable to chronic ischemic injury. The white matter rarefaction had the greatest dimension, making it the most likely histopathological correlate for the ~ 2 mm diameter MRI lesion. Immunohistochemistry for phosphorylated tau revealed no evidence of CTE neuropathology in routine, whole-mount, or image-guided histopathological analyses.

Discussion

The LETBI project represents a systematic effort to characterize the clinical and pathological late effects of TBI with the goal of identifying *in vivo* signatures of postmortem pathology. This multimodal approach to integrating histopathology, *ex vivo* MRI, *in vivo* MRI, and cognitive-behavioral data in the LETBI project is based upon the premise that postmortem neuropathological data in well-characterized clinical samples are essential to elucidate the pathogenesis of post-TBI neurodegeneration, define relationships between TBI neuropathology and clinical phenotypes of commonly diagnosed neurodegenerative conditions, identify risk factors, and develop diagnostic and therapeutic strategies. Here, we describe the study methods and demonstrate feasibility and proof of concept using data collected from the first participant to undergo our full *ex vivo* protocol. This unselected case demonstrates the utility of this approach to characterizing the late effects of TBI even in a patient who had normal cognition and functional independence until her early 80s after sustaining two TBIs with LOC. Our methods are well suited to accommodate the complexity of distinguishing the late effects of TBI in older adults, in whom path-

ological abnormalities are the norm rather than the exception, and in whom the links between pathological abnormalities and clinical manifestations is much weaker than it is among younger individuals. As the LETBI sample grows, our unbiased case selection and comprehensive *in vivo* and *ex vivo* characterization may facilitate identification of markers of resilience to the late effects of TBI, which in turn may inform treatment strategies.

An innovation in the LETBI project is the acquisition of *ex vivo* MRI data to serve as a methodological bridge linking gold standard histopathological data to *in vivo* MRI and cognitive-behavioral data. As seen in our index case, *ex vivo* MRI is able to detect lesions not seen by *in vivo* MRI, and provides a three-dimensional whole-brain view of pathological lesions not sampled during a histopathological evaluation. Identification of lesions on *ex vivo* MRI enables targeted histopathological sampling of the brain tissue. Similarly, our advanced *ex vivo*-to-*in vivo* MRI co-registration technique allows precise localization of the neuroanatomic coordinates of a lesion on the *in vivo* MRI dataset, enabling analysis of its *in vivo* MRI signal characteristics and its clinical correlates. The approach presented here thus represents an opportunity to link the microscope to the bedside using *ex vivo* MRI as an intermediate.

The LETBI project also aims to balance the complementary approaches of hypothesis testing and hypothesis generation. We designed the study to accommodate the need for prospective, unbiased analyses that control for exposures that may confound the association between TBI and neurodegeneration (e.g. substance abuse), while fully recognizing that current knowledge about the *in vivo* biomarkers and histopathological signatures of post-traumatic neurodegeneration is insufficient. Given recent evidence that post-traumatic neurodegeneration may be a polyopathy^{4,6} with histopathological features of AD, PD, CTE, and vascular lesions, we designed the LETBI project to allow for the identification of different types of

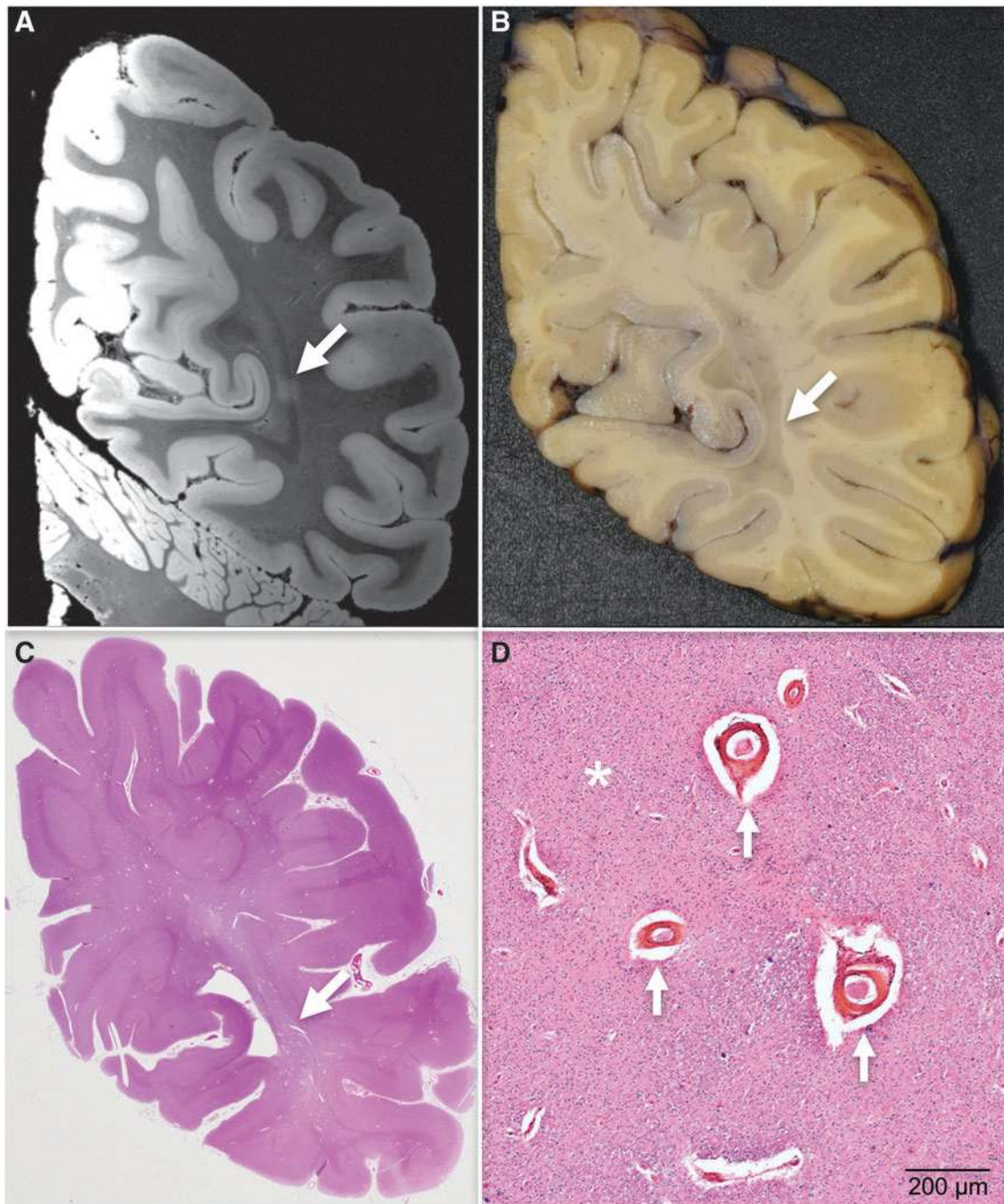


FIG. 9. Targeted whole-mount histopathological analysis based on *ex vivo* magnetic resonance imaging (MRI) lesion localization. The punctate hyperintense lesion in the occipital white matter identified on *ex vivo* 7 Tesla (7T) MRI is first localized in the coronal plane (A, white arrow), because this is the plane in which the gross pathological specimen is cut into ~1.5 cm thick slabs. During an audiovisual consensus teleconference, the precise anatomic coordinates of the lesion seen on *ex vivo* 7T MRI are compared with surface landmarks seen on the serial coronal slabs using high resolution photographs of the tissue slabs. The investigators of the Late Effects of Traumatic Brain Injury study select a slab for whole-mount analysis (B) based upon its correspondence with the coronal MRI image that contained the lesion. Whole-mount analysis is then performed on this coronal slab (C), enabling targeted histopathological analysis (D) of the lesion identified on *ex vivo* MRI. This histopathological analysis revealed enlarged perivascular spaces (arrows), corpora amylacea, and white matter rarefaction (asterisk). A single pathological process, ischemia, is the likely cause of these pathological findings. Color image is available online at www.liebertpub.com/neu

pathologies. Specifically, the *ex vivo* MRI protocol involves multiple contrasts, and the histopathological protocol involves multiple immunostains. The importance of this balanced approach to hypothesis testing and hypothesis generation is evidenced by the results from the index case. On the one hand, the results of the

occipital lesion analysis support the hypothesis that TBI is associated with pathologic abnormalities that correlate with ultra-high resolution *ex vivo* MRI biomarkers and *in vivo* MRI biomarkers. On the other hand, the absence of clinical signs of dementia and the absence of pathological features of neurodegeneration despite six

TBIs provide a basis to test future hypotheses about mechanisms of resilience to post-traumatic neurodegeneration.

Importantly, participants in the LETBI project have a history of TBI but do not necessarily have clinically significant deficits or evidence of decline. Enrollment of patients prior to symptom onset allows us to comprehensively characterize at-risk individuals before the onset of late effects of TBI. Although many long-term survivors of TBI experience dramatic functional decline from a previously achieved level of recovery, others remain stable or even continue to recover for years after injury.⁴⁸ As seen in the index case reported here, a history of multiple injuries sustained across the lifespan does not preclude high level functioning into late life and minimal postmortem evidence of traumatic injury. Our choice to demonstrate the LETBI project methods using this case, the first to undergo the full LETBI *ex vivo* protocol, is consistent with the LETBI investigative team's commitment to share positive and negative findings with equal transparency in an effort to fully elucidate the late effects of TBI.

There are several limitations to the LETBI study that warrant consideration. First, while the prospective enrollment of at-risk asymptomatic individuals with prior TBI reduces selection bias, this approach also necessitates a larger sample size and longer duration of follow-up to make robust inferences about mechanistic links between TBI and neurodegeneration. Other studies have made major contributions to characterizing post-traumatic pathology by gathering postmortem brain specimens from symptomatic individuals with specific types of TBI exposure (e.g. athletes with repetitive head trauma).⁴⁹ The LETBI study similarly aims to characterize post-traumatic neuropathology, but the complementary goal of identifying *in vivo* markers of this pathology necessitates a concerted long-term effort for prospective clinical data collection. Relatedly, early hypothesis testing will be restricted to analyses that are appropriately powered as the sample size grows with continued enrollment. Second, the control cases in the LETBI study undergo only the *ex vivo* MRI and histopathology protocols, and comprehensive clinical data are not routinely available. The control cases also originate from separate cohorts, which introduces a potential source of sampling bias. Third, the LETBI study does not leverage recent advances in structural and functional MRI.^{39,50} Like other ongoing multi-institutional TBI studies,¹³ the LETBI study prioritizes harmonization and standardization of *in vivo* MRI protocols across sites, recognizing that there is an inherent trade-off between standardization and innovation.

Conclusions

Postmortem data gathered from well-characterized clinical cohorts are essential to characterize the pathological substrate associated with the late effects of TBI and to determine the clinical signatures of post-TBI neurodegeneration. Prospective clinical studies with autopsy end-points minimize selection bias and address the many factors that may impact associations between TBI exposure and neurodegenerative pathology.⁵¹ The methods described here are designed to advance scientific knowledge about the pathological substrates and clinical phenotypes associated with post-traumatic neurodegeneration and resilience, while also facilitating discovery of novel histopathological and neuroimaging biomarkers for future hypothesis testing. The LETBI project uses multimodal methods to link *in vivo* imaging and neurobehavioral data with *ex vivo* imaging and histology, with a goal of facilitating prevention, diagnosis and treatment of post-TBI neurodegeneration during life.

Acknowledgments

We thank Michelle Siciliano, Gregory Tirrell, Sebastian Valentin, Terrence Ott, Vahram Haroutunian, and Maxwell Bustamante for assistance in obtaining and processing brain specimens; William Lee for providing database management and data sharing support; and Thomas Benner for implementation of the DWSSFP sequence for *ex vivo* MRI. We would like to acknowledge Dylan Tisdall and Andre van der Kouwe (Athinoula A. Martinos Center for Biomedical Imaging) and Himanshu Bhat (Siemens Medical Center) for the provision of WIP711D (vNav Motion-Corrected Multiecho MPRAGE) used to acquire MEMPRAGE data. The LETBI Project is supported by the National Institutes of Health/ National Institute for Neurological Disorders and Stroke and National Institute of Child Health and Development (U01 NS086625). This research also utilized resources provided by the National Center for Research Resources (U24 RR021382), the National Institute for Biomedical Imaging and Bioengineering (P41EB015896, R01EB006758, R21EB018907, R01EB019956, 1R01EB023281), the National Institute on Aging (AG022381, 5R01AG008122, R01 AG016495, 5R01AG008122, U01AG006781, R21AG046657, P41RR014075, P50AG005136), the National Center for Alternative Medicine (RC1 AT005728-01), the National Institute for Neurological Disorders and Stroke (K23NS094538, R01NS052585-01, 1R21NS072652-01, 1R01NS070963, R01NS083534, 5U01NS086625), the Eunice Kennedy Shriver National Institute of Child Health and Human Development (1K01HD074651, R01HD071664), the National Institute on Disability Independent Living and Rehabilitation Research (H133B040033), and the Centers for Disease Control and Prevention (1R49CE001171). Additional support was provided by the NIH Blueprint for Neuroscience Research (5U01-MH093765), part of the multi-institutional Human Connectome Project. This research also utilized resources provided by National Institutes of Health shared instrumentation grants 1S10RR023401, 1S10RR019307, and 1S10RR023043. Additional support for this project comes from the American Academy of Neurology/American Brain Foundation, the James S. McDonnell Foundation, the Nancy and Buster Alvord Endowment, institutional funds from the University of Washington School of Medicine, and the Seton Brain Research Fund. The opinions expressed herein are those of the authors and are not necessarily representative of those of the Uniformed Services University of the Health Sciences, the Department of Defense, the United States Army, Navy or Air Force, or of any other agency or component of the United States government.

Author Disclosure Statement

No competing financial interests exist.

Dr. Fischl and Mr. Tirrell have financial interest in CorticoMetrics, a company whose medical pursuits focus on brain imaging and measurement technologies. Their interests were reviewed and are managed by Massachusetts General Hospital and Partners HealthCare in accordance with their conflict of interest policies.

References

1. Smith, D.H., Johnson, V.E., and Stewart, W. (2013). Chronic neuropathologies of single and repetitive TBI: substrates of dementia? *Nature Rev. Neurol.* 9, 211–221.
2. Johnson, V.E., Stewart, W., and Smith, D.H. (2010). Traumatic brain injury and amyloid-beta pathology: a link to Alzheimer's disease? *Nat. Rev. Neurol.* 11, 361–370.

3. McKee, A.C., Stein, T.D., Nowinski, C.J., Stern, R.A., Daneshvar, D.H., Alvarez, V.E., Lee, H.S., Hall, G., Wojtowicz, S.M., Baugh, C.M., Riley, D.O., Kubilus, C.A., Cormier, K.A., Jacobs, M.A., Martin, B.R., Abraham, C.R., Ikezu, T., Reichard, R.R., Wolozin, B.L., Budson, A.E., Goldstein, L.E., Kowall, N.W., and Cantu, R.C. (2013). The spectrum of disease in chronic traumatic encephalopathy. *Brain* 136, 43–64.
4. Crane, P.K., Gibbons, L.E., Dams-O'Connor, K., Trittschuh, E., Leverenz, J.B., Keene, C.D., Sonnen, J., Montine, T.J., Bennett, D.A., Leurgans, S., Schneider, J.A., and Larson, E.B. (2016). Association of traumatic brain injury with late-life neurodegenerative conditions and neuropathologic findings. *JAMA Neurol.* 73, 1062–1069.
5. Health IOM COGWA (2008). Long-term consequences of traumatic brain injury. In: *Gulf War and Health*. National Academies Press: Washington, DC.
6. Kenney, K., Iacono, D., Edlow, B.L., Katz, D.I., Diaz-Arrastia, R., Dams-O'Connor, K., Daneshvar, D.H., Stevens, A., Moreau, A.L., Tirrell, L.S., Varjabedian, A., Yendiki, A., van der Kouwe, A., Marcyam, A., McNab, J.A., Gordon, W.A., Fischl, B., McKee, A.C., and Perl, D.P. (2017). Dementia after moderate-severe traumatic brain injury: coexistence of multiple proteinopathies. *J. Neuropathol. Exp. Neurol.* 77, 50–63.
7. Wilson, L., Stewart, W., Dams-O'Connor, K., Diaz-Arrastia, R., Horton, L., Menon, D.K., and Polinder, S. (2017). The chronic and evolving neurological consequences of traumatic brain injury. *Lancet Neurol.* 16, 813–825.
8. Dams-O'Connor, K., Guetta, G., Hahn-Ketter, A.E., and Fedor, A. (2016). Traumatic brain injury as a risk factor for Alzheimer's disease: current knowledge and future directions. *Neurodegener. Dis. Manag.* 6, 417–429.
9. Kukull, W.A., Higdon, R., Bowen, J.D., McCormick, W.C., Teri, L., Schellenberg, G.D., van Belle, G., Jolley, L., and Larson, E.B. (2002). Dementia and Alzheimer disease incidence: a prospective cohort study. *Arch. Neurol.* 59, 1737–1746.
10. Dijkers, M.P., Harrison-Felix, C., and Marwitz, J.H. (2010). The traumatic brain injury model systems: history and contributions to clinical service and research. *J. Head Trauma Rehabil.* 25, 81–91.
11. American Congress of Rehabilitation Medicine (1993). Definition of mild traumatic brain injury. *J. Head Trauma Rehabil.* 8, 86–87.
12. Maas, A.I., Harrison-Felix, C.L., Menon, D., Adelson, P.D., Balkin, T., Bullock, R., Engel, D.C., Gordon, W., Orman, J.L., Lew, H.L., Robertson, C., Temkin, N., Valadka, A., Verfaellie, M., Wainwright, M., Wright, D.W., and Schwab, K. (2010). Common data elements for traumatic brain injury: recommendations from the interagency working group on demographics and clinical assessment. *Arch. Phys. Med. Rehabil.* 91, 1641–1649.
13. Yue, J.K., Vassar, M.J., Lingsma, H.F., Cooper, S.R., Okonkwo, D.O., Valadka, A.B., Gordon, W.A., Maas, A.I., Mukherjee, P., Yuh, E.L., Puccio, A.M., Schnyer, D.M., and Manley, G.T.; TRACK-TBI Investigators. (2013). Transforming research and clinical knowledge in traumatic brain injury pilot: multicenter implementation of the common data elements for traumatic brain injury. *J. Neurotrauma* 30, 1831–1844.
14. van der Kouwe, A.J., Benner, T., Salat, D.H., and Fischl, B. (2008). Brain morphometry with multiecho MPRAGE. *Neuroimage* 40, 559–569.
15. Haacke, E.M., Xu, Y., Cheng, Y.C., and Reichenbach, J.R. (2004). Susceptibility weighted imaging (SWI). *Magn. Reson. Med.* 52, 612–618.
16. Mori, S., Crain, B.J., Chacko, V.P., and van Zijl, P.C. (1999). Three-dimensional tracking of axonal projections in the brain by magnetic resonance imaging. *Ann. Neurol.* 45, 265–269.
17. Behrens, T.E., Woolrich, M.W., Jenkinson, M., Johansen-Berg, H., Nunes, R.G., Clare, S., Matthews, P.M., Brady, J.M., and Smith, S.M. (2003). Characterization and propagation of uncertainty in diffusion-weighted MR imaging. *Magn. Reson. Med.* 50, 1077–1088.
18. Biswal, B.B., Mennes, M., Zuo, X.N., Gohel, S., Kelly, C., Smith, S.M., Beckmann, C.F., Adelstein, J.S., Buckner, R.L., Colcombe, S., Dogonowski, A.M., Ernst, M., Fair, D., Hampson, M., Hoptman, M.J., Hyde, J.S., Kiviniemi, V.J., Kottler, R., Li, S.J., Lin, C.P., Lowe, M.J., Mackay, C., Madden, D.J., Madsen, K.H., Margulies, D.S., Mayberg, H.S., McMahon, K., Monk, C.S., Mostofsky, S.H., Nagel, B.J., Pekar, J.J., Peltier, S.J., Petersen, S.E., Riedl, V., Rombouts, S.A., Rypma, B., Schlaggar, B.L., Schmidt, S., Seidler, R.D., Siegle, G.J., Sorg, C., Teng, G.J., Vejjola, J., Villringer, A., Walter, M., Wang, L., Weng, X.C., Whitfield-Gabrieli, S., Williamson, P., Windischberger, C., Zang, Y.F., Zhang, H.Y., Castellanos, F.X., and Milham, M.P. (2010). Toward discovery science of human brain function. *Proc. Natl. Acad. Sci. U. S. A.* 107, 4734–4739.
19. Haacke, E.M., Duhaime, A.C., Gean, A.D., Riedy, G., Wintermark, M., Mukherjee, P., Brody, D.L., DeGraba, T., Duncan, T.D., Elovic, E., Hurley, R., Latour, L., Smirniotopoulos, J.G., and Smith, D.H. (2010). Common data elements in radiologic imaging of traumatic brain injury. *J. Magn. Reson. Imaging* 32, 516–543.
20. Duhaime, A.C., Gean, A.D., Haacke, E.M., Hicks, R., Wintermark, M., Mukherjee, P., Brody, D., Latour, L., and Riedy, G. (2010). Common data elements in radiologic imaging of traumatic brain injury. *Arch. Phys. Med. Rehabil.* 91, 1661–1666.
21. Yendiki, A., Panneck, P., Srinivasan, P., Stevens, A., Zollei, L., Augstinack, J., Wang, R., Salat, D., Ehrlich, S., Behrens, T., Jbabdi, S., Gollub, R., and Fischl, B. (2011). Automated probabilistic reconstruction of white-matter pathways in health and disease using an atlas of the underlying anatomy. *Front. Neuroinform.* 5, 23.
22. Smith, S.M., Jenkinson, M., Woolrich, M.W., Beckmann, C.F., Behrens, T.E., Johansen-Berg, H., Bannister, P.R., De Luca, M., Drobnjak, I., Flitney, D.E., Niazy, R.K., Saunders, J., Vickers, J., Zhang, Y., De Stefano, N., Brady, J.M., and Matthews, P.M. (2004). Advances in functional and structural MR image analysis and implementation as FSL. *Neuroimage* 23 Suppl 1, S208–S219.
23. Whitfield-Gabrieli, S. and Nieto-Castanon, A. (2012). Conn: a functional connectivity toolbox for correlated and anticorrelated brain networks. *Brain Connect.* 2, 125–141.
24. Yuh, E.L., Mukherjee, P., Lingsma, H.F., Yue, J.K., Ferguson, A.R., Gordon, W.A., Valadka, A.B., Schnyer, D.M., Okonkwo, D.O., Maas, A.I., and Manley, G.T.; TRACK-TBI Investigators. (2013). Magnetic resonance imaging improves 3-month outcome prediction in mild traumatic brain injury. *Ann. Neurol.* 73, 224–235.
25. Saver, J.L., Warach, S., Janis, S., Odenkirchen, J., Becker, K., Benavente, O., Broderick, J., Dromerick, A.W., Duncan, P., Elkind, M.S., Johnston, K., Kidwell, C.S., Meschia, J.F., and Schwamm, L.; National Institute of Neurological Disorders and Stroke (NINDS) Stroke Common Data Element Working Group. (2012). Standardizing the structure of stroke clinical and epidemiologic research data: the National Institute of Neurological Disorders and Stroke (NINDS) Stroke Common Data Element (CDE) project. *Stroke* 43, 967–973.
26. Dams-O'Connor, K., Cantor, J.B., Brown, M., Dijkers, M.P., Spielman, L.A., and Gordon, W.A. (2014). Screening for traumatic brain injury: findings and public health implications. *J. Head Trauma Rehabil.* 29, 479–489.
27. Montine, T.J., Phelps, C.H., Beach, T.G., Bigio, E.H., Cairns, N.J., Dickson, D.W., Duyckaerts, C., Frosch, M.P., Masliah, E., Mirra, S.S., Nelson, P.T., Schneider, J.A., Thal, D.R., Trojanowski, J.Q., Vinters, H.V., and Hyman, B.T.; National Institute on Aging; Alzheimer's Association. (2012). National Institute on Aging-Alzheimer's Association guidelines for the neuropathologic assessment of Alzheimer's disease: a practical approach. *Acta Neuropathol.* 123, 1–11.
28. Hyman, B.T., Phelps, C.H., Beach, T.G., Bigio, E.H., Cairns, N.J., Carrillo, M.C., Dickson, D.W., Duyckaerts, C., Frosch, M.P., Masliah, E., Mirra, S.S., Nelson, P.T., Schneider, J.A., Thal, D.R., Thies, B., Trojanowski, J.Q., Vinters, H.V., and Montine, T.J. (2012). National Institute on Aging-Alzheimer's Association guidelines for the neuropathologic assessment of Alzheimer's disease. *Alzheimers Dement.* 8, 1–13.
29. Sonnen, J.A., Larson, E.B., Crane, P.K., Haneuse, S., Li, G., Schellenberg, G.D., Craft, S., Leverenz, J.B., and Montine, T.J. (2007). Pathological correlates of dementia in a longitudinal, population-based sample of aging. *Ann. Neurol.* 62, 406–413.
30. Bettcher, B.M., Ard, M.C., Reed, B.R., Benitez, A., Simmons, A., Larson, E.B., Sonnen, J.A., Montine, T.J., Li, G., Keene, C.D., Crane, P.K., and Mungas, D. (2017). Association between cholesterol exposure and neuropathological findings: the ACT Study. *J. Alzheimers Dis.* 59, 1307–1315.
31. Postupna, N., Latimer, C.S., Larson, E.B., Sherfield, E., Paladin, J., Shively, C.A., Jorgensen, M.J., Andrews, R.N., Kaplan, J.R., Crane, P.K., Montine, K.S., Craft, S., Keene, C.D., and Montine, T.J. (2017). Human striatal dopaminergic and regional serotonergic synaptic degeneration with lewy body disease and inheritance of APOE epsilon4. *Am. J. Pathol.* 187, 884–895.
32. Postupna, N., Rose, S.E., Bird, T.D., Gonzalez-Cuyar, L.F., Sonnen, J.A., Larson, E.B., Keene, C.D., and Montine, T.J. (2012). Novel

- antibody capture assay for paraffin-embedded tissue detects widespread amyloid beta and paired helical filament-tau accumulation in cognitively normal older adults. *Brain Pathol.* 22, 472–484.
33. Postupna, N., Keene, C.D., Crane, P.K., Gonzalez-Cuyar, L.F., Sonnen, J.A., Hewitt, J., Rice, S., Howard, K., Montine, K.S., Larson, E.B., and Montine, T.J. (2015). Cerebral cortical Abeta42 and PHF-tau in 325 consecutive brain autopsies stratified by diagnosis, location, and APOE. *J. Neuropathol. Exp. Neurol.* 74, 100–109.
 34. Fischl, B., Salat, D.H., van der Kouwe, A.J., Makris, N., Segonne, F., Quinn, B.T., and Dale, A.M. (2004). Sequence-independent segmentation of magnetic resonance images. *Neuroimage* 23 Suppl 1, S69–S84.
 35. McNab, J.A., Jbabdi, S., Deoni, S.C., Douaud, G., Behrens, T.E., and Miller, K.L. (2009). High resolution diffusion-weighted imaging in fixed human brain using diffusion-weighted steady state free precession. *Neuroimage* 46, 775–785.
 36. Deoni, S.C., Peters, T.M., and Rutt, B.K. (2005). High-resolution T1 and T2 mapping of the brain in a clinically acceptable time with DESPOT1 and DESPOT2. *Magn. Reson. Med.* 53, 237–241.
 37. Fischl, B., Sereno, M.I., Tootell, R.B., and Dale, A.M. (1999). High-resolution intersubject averaging and a coordinate system for the cortical surface. *Hum. Brain Mapp.* 8, 272–284.
 38. Fischl, B. (2012). FreeSurfer. *Neuroimage* 62, 774–781.
 39. McNab, J.A., Edlow, B.L., Witzel, T., Huang, S.Y., Bhat, H., Heberlein, K., Keil, B., Cohen-Adad, J., Tisdall, M.D., Folkerth, R.D., Kinney, H.C., and Wald, L.L. (2013). The human connectome project and beyond: Initial applications of 300 mT/m gradients. *NeuroImage* 80, 234–445.
 40. Catani, M. and Thiebaut de Schotten, M. (2008). A diffusion tensor imaging tractography atlas for virtual in vivo dissections. *Cortex* 44, 1105–1132.
 41. Edlow, B.L., Haynes, R.L., Takahashi, E., Klein, J.P., Cummings, P., Benner, T., Greer, D.M., Greenberg, S.M., Wu, O., Kinney, H.C., and Folkerth, R.D. (2013). Disconnection of the ascending arousal system in traumatic coma. *J. Neuropathol. Exp. Neurol.* 72, 505–523.
 42. Edlow, B.L., Takahashi, E., Wu, O., Benner, T., Dai, G., Bu, L., Grant, P.E., Greer, D.M., Greenberg, S.M., Kinney, H.C., and Folkerth, R.D. (2012). Neuroanatomic connectivity of the human ascending arousal system critical to consciousness and its disorders. *J. Neuropathol. Exp. Neurol.* 71, 531–546.
 43. Edlow, B.L., McNab, J.A., Witzel, T., and Kinney, H.C. (2016). The structural connectome of the human central homeostatic network. *Brain Connect.* 6, 187–200.
 44. Postelnicu, G., Zollei, L., and Fischl, B. (2009). Combined volumetric and surface registration. *IEEE Trans. Med. Imaging* 28, 508–522.
 45. Sours, C., Hinds, S.R., 2nd, McKee, A.C., Perl, D.P., and Leggieri, M.J., Jr. (2017). Brain banks and tissue repositories for blast-related chronic traumatic encephalopathy research. *J. Neurotrauma* 34, S4–S5.
 46. Thal, D.R., Rub, U., Orantes, M., and Braak, H. (2002). Phases of A beta-deposition in the human brain and its relevance for the development of AD. *Neurology* 58, 1791–1800.
 47. Crary, J.F., Trojanowski, J.Q., Schneider, J.A., Abisambra, J.F., Abner, E.L., Alafuzoff, I., Arnold, S.E., Attems, J., Beach, T.G., Bigio, E.H., Cairns, N.J., Dickson, D.W., Gearing, M., Grinberg, L.T., Hof, P.R., Hyman, B.T., Jellinger, K., Jicha, G.A., Kovacs, G.G., Knopman, D.S., Kofler, J., Kukull, W.A., Mackenzie, I.R., Masliah, E., McKee, A., Montine, T.J., Murray, M.E., Neltner, J.H., Santa-Maria, I., Seeley, W.W., Serrano-Pozo, A., Shelanski, M.L., Stein, T., Takao, M., Thal, D.R., Toledo, J.B., Troncoso, J.C., Vonsattel, J.P., White, C.L., 3rd, Wisniewski, T., Woltjer, R.L., Yamada, M., and Nelson, P.T. (2014). Primary age-related tauopathy (PART): a common pathology associated with human aging. *Acta Neuropathol.* 128, 755–766.
 48. Corrigan, J.D., Cuthbert, J.P., Harrison-Felix, C., Whiteneck, G.G., Bell, J.M., Miller, A.C., Coronado, V.G., and Pretz, C.R. (2014). US population estimates of health and social outcomes 5 years after rehabilitation for traumatic brain injury. *J. Head Trauma Rehabil.* 29, E1–E9.
 49. Mez, J., Daneshvar, D.H., Kiernan, P.T., Abdolmohammadi, B., Alvarez, V.E., Huber, B.R., Alosco, M.L., Solomon, T.M., Nowinski, C.J., McHale, L., Cormier, K.A., Kubilus, C.A., Martin, B.M., Murphy, L., Baugh, C.M., Montenigro, P.H., Chaisson, C.E., Tripodis, Y., Kowall, N.W., Weuve, J., McClean, M.D., Cantu, R.C., Goldstein, L.E., Katz, D.I., Stern, R.A., Stein, T.D., and McKee, A.C. (2017). Clinicopathological evaluation of chronic traumatic encephalopathy in players of American football. *JAMA* 318, 360–370.
 50. Smith, S.M., Beckmann, C.F., Andersson, J., Auerbach, E.J., Bijsterbosch, J., Douaud, G., Duff, E., Feinberg, D.A., Griffanti, L., Harms, M.P., Kelly, M., Laumann, T., Miller, K.L., Moeller, S., Petersen, S., Power, J., Salimi-Khorshidi, G., Snyder, A.Z., Vu, A.T., Woolrich, M.W., Xu, J., Yacoub, E., Ugurbil, K., Van Essen, D.C., and Glasser, M.F.; WU-Minn HCP Consortium. (2013). Resting-state fMRI in the Human Connectome Project. *Neuroimage* 80, 144–168.
 51. Mahar, I., Alosco, M.L., and McKee, A.C. (2017). Psychiatric phenotypes in chronic traumatic encephalopathy. *Neurosci. Biobehav. Rev.* 83, 622–630.
 52. Wechsler, D. (2008). Wechsler Adult Intelligence Scale–Fourth Edition (WAIS–IV). Pearson: San Antonio, TX.
 53. Tombaugh, T.N. (2004). Trail Making Test A and B: normative data stratified by age and education. *Arch. Clin. Neuropsychol.* 19, 203–214.
 54. Delis, D., Kramer, J., Kaplan, E. and Ober, B. (2000). California Verbal Learning Test: Second Edition. Psychological Corporation: San Antonio, TX.
 55. Delis, D.C., Kramer, J.H., Kaplan, E. and Ober, B.A. (1987). California Verbal Learning Test: Adult Version Manual. The Psychological Corporation: San Antonio, TX.
 56. Wechsler, D. (1987). WMS-R: Wechsler Memory Scale–Revised manual. Psychological Corp., Harcourt Brace Jovanovich: San Antonio, TX.
 57. Meyers, J. and Meyers, K. Rey complex figure test and recognition trial: Professional manual. PAR, Inc.
 58. Benton, A. and Hamsher, K. (1989). Multilingual Aphasia Examination. AJA Associates: Iowa City.
 59. Cella, D., Lai, J.S., Nowinski, C.J., Victorson, D., Peterman, A., Miller, D., Bethoux, F., Heinemann, A., Rubin, S., Cavazos, J.E., Reder, A.T., Sufit, R., Simuni, T., Holmes, G.L., Siderowf, A., Wojna, V., Bode, R., McKinney, N., Podrabsky, T., Wortman, K., Choi, S., Gershon, R., Rothrock, N. and Moy, C. (2012). Neuro-QOL: brief measures of health-related quality of life for clinical research in neurology. *Neurology* 78, 1860–1867.
 60. (2009). Traumatic Brain Injury Model Systems National Database Syllabus. Traumatic Brain Injury Model Systems National Data and Statistical Center.
 61. Diener, E., Emmons, R.A., Larsen, R.J. and Griffin, S. (1985). The Satisfaction With Life Scale. *J. Pers. Assess.* 49, 71–75.
 62. Ware, J.E. and Kosinski, M. (2001). SF-36 Physical and Mental Health Summary Scales: A Manual for Users of Version 1. Vol 2nd. Quality Metric, Inc.
 63. Ware, J.E., Jr. and Sherbourne, C.D. (1992). The MOS 36-item short-form health survey (SF-36). I. Conceptual framework and item selection. *Med. Care* 30, 473–483.
 64. Hays, R., Sherbourne, C.D., Mazel, R.M. (1995). User’s Manual for the Medical Outcomes Study (MOS) Core Measures of Health-Related Quality of Life. RAND: Santa Monica, CA.
 65. Goetz, C.G., Tilley, B.C., Shaftman, S.R., Stebbins, G.T., Fahn, S., Martinez-Martin, P., Poewe, W., Sampaio, C., Stern, M.B., Dodel, R., Dubois, B., Holloway, R., Jankovic, J., Kulisevsky, J., Lang, A.E., Lees, A., Leurgans, S., LeWitt, P.A., Nyenhuis, D., Olanow, C.W., Rascol, O., Schrag, A., Teresi, J.A., van Hilten, J.J. and LaPelle, N. (2008). Movement Disorder Society-sponsored revision of the Unified Parkinson’s Disease Rating Scale (MDS-UPDRS): Scale presentation and clinimetric testing results. *Mov. Disord.* 23, 2129–2170.
 66. Patton, J.H., Stanford, M.S. and Barratt, E.S. (1995). Factor structure of the Barratt impulsiveness scale. *J. Clin. Psychol.* 51, 768–769–774.
 67. Coccaro, E.F., Berman, M.E. and Kavoussi, R.J. (1997). Assessment of life history of aggression: development and psychometric characteristics. *Psychiatry Res.* 73, 147–157.
 68. Maas, A.I., Harrison-Felix, C.L., Menon, D., Adelson, P.D., Balkin, T., Bullock, R., Engel, D.C., Gordon, W., Langlois-Orman, J., Lew, H.L., Robertson, C., Temkin, N., Valadka, A., Verfaellie, M., Wainwright, M., Wright, D.W. and Schwab, K. (2011). Standardizing data collection in traumatic brain injury. *J. Neurotrauma* 28, 177–187.
 69. Ryff, C., Almeida, D.M., Ayanian, J., Carr, D.S., Cleary, P.D., Coe, C., Davidson, R., Krueger, R.F., Lachman, M.E., Marks, N.F., Mroczek, D.K., Seeman, T., Seltzer, M.M., Singer, B.H., Sloan, R.P., Tun, P.A., Weinstein, M. and Williams, D. (2012). National Survey of Midlife Development in the United States (MIDUS II), 2004–2006. Inter-university Consortium for Political and Social Research (ICPSR).

70. Hibbard, M., Brown, M. and Gordon, W. (1999). Brain Injury Screening Questionnaire. User's Manual. Research and Training Center on Community Integration of Individual with Traumatic Brain Injury, Department of Rehabilitation Medicine, Mount Sinai School of Medicine: New York.
71. Gordon, W.A., Brown, M. and Hibbard, M. (1999). Brain Injury Screening Questionnaire. Research and Training Center on Community Integration of Individual with Traumatic Brain Injury, Department of Rehabilitation Medicine, Mount Sinai School of Medicine: New York.
72. Guralnik, J.M., Simonsick, E.M., Ferrucci, L., Glynn, R.J., Berkman, L.F., Blazer, D.G., Scherr, P.A. and Wallace, R.B. (1994). A short physical performance battery assessing lower extremity function: association with self-reported disability and prediction of mortality and nursing home admission. *Journal of gerontology* 49, M85-94.
73. Humeniuk, R., Ali, R., Babor, T.F., Farrell, M., Formigoni, M.L., Jittiwutikarn, J., de Lacerda, R.B., Ling, W., Marsden, J., Monteiro, M., Nhwatiwa, S., Pal, H., Poznyak, V. and Simon, S. (2008). Validation of the Alcohol, Smoking And Substance Involvement Screening Test (ASSIST). *Addiction* 103, 1039-1047.
74. Group, W.A.W. (2002). The Alcohol, Smoking and Substance Involvement Screening Test (ASSIST): development, reliability and feasibility. *Addiction* 97, 1183-1194.

Address correspondence to:
Kristen Dams-O'Connor, PhD
Brain Injury Research Center
Department of Rehabilitation Medicine
Icahn School of Medicine at Mount Sinai
Box 1163, One Gustave L. Levy Place
New York, NY 10029

E-mail: kristen.dams-o'connor@mountsinai.org